

# The effects of adsorbed water on dynamic mechanical properties of wood

Eiichi Obataya<sup>a,\*</sup>, Misato Norimoto<sup>a</sup> and Joseph Gril<sup>b</sup>

<sup>a</sup>Wood Research Institute, Kyoto University, Uji, Kyoto 611, Japan

<sup>b</sup>Laboratoire de Mécanique et Génie Civil, Université de Montpellier 2, 34095 Montpellier Cedex 5, France

(Received 29 August 1996; revised 23 May 1997; accepted 15 August 1997)

The storage modulus and the loss tangent of Sitka spruce wood (*Picea Sitchensis*) in the longitudinal direction at various moisture contents were measured at 20°C, and the effect of adsorbed water was investigated by using a uniaxial rheological model to eliminate the contribution of matrix swelling. The largest value for Young's modulus of matrix was obtained at around 8% moisture content. The rearrangement of matrix molecules accompanied by the adsorption of hydrated water increased the value of Young's modulus up to about 8% moisture content, whereas the plasticization of matrix molecules by the adsorption of dissolved water decreased it at above 8% moisture content. The loss tangent of matrix had two peaks at ~1% and 20% moisture contents. It was considered that the former was due to the motion of the adsorbed water itself and the latter to the relaxation related to the micro-Brownian motion of matrix substances, especially hemicelluloses. © 1998 Elsevier Science Ltd. All rights reserved.

(Keywords: wood; dynamic properties; moisture content)

## INTRODUCTION

Numerous studies have been made on the moisture dependence of the dynamic mechanical properties of wood<sup>1–6</sup>, especially in the longitudinal direction<sup>1–4</sup>. Although such a dependence has been attributed to the effect of adsorbed water on the structure of amorphous matrix substances in the cell wall, there is one further effect of the adsorbed water that we must not ignore: swelling. At the macromolecular level (1–100 nm), wood material can be schematically described as a two phase composite of elastic fibrils consisting of cellulose and a part of hemicellulose, and a viscoelastic matrix substance consisting of lignin and the remaining part of hemicellulose. The dynamic properties of wood are mainly determined by both the dynamic properties and the volume fractions of these constituents. The changes in the dynamic properties of wood with varying moisture content may reflect changes not only in matrix structure but also in the volume fractions. The question of how to quantify the dynamic properties of matrix remains.

Although the theoretical analyses of the elastic properties of wood by using structural models have been attempted by many researchers<sup>7–11</sup>, there are few papers for the viscoelastic ones. In our previous study<sup>12</sup>, the effects of chemical treatment on the dynamic properties of matrix were analysed by using a unidirectional rheological model. However, the assumption that fibrils run along the longitudinal direction of wood predicted a value of storage modulus much larger than that measured at high moisture contents. Consequently, the estimate of storage modulus of

matrix from the model was unrealistic at high moisture contents. In the present study, we will try to estimate the dynamic properties of matrix by using a uniaxial model in which the angle of fibrils will be taken into consideration and to discuss the effects of adsorbed water on the matrix.

## EXPERIMENT

Sitka spruce (*Picea Sitchensis* Carr.) specimens, 150 mm (L = longitudinal direction) (15 mm (R = radial direction) (1.8 mm (T = tangential direction), with specific gravities ( $\gamma$ ) ranging from 0.42 to 0.47, were used. The resonant frequencies ( $f$ : Hz) and the logarithmic decrement ( $\lambda$ ) of the first vibration mode were detected by a free-free beam flexural vibration method<sup>13</sup> as shown in *Figure 1*. The storage modulus ( $E'$ ) and the loss tangent ( $\tan\delta$ ) were calculated from  $f$  and  $\lambda$ .

The specimens were dried for 3 days over dry silica gel at room temperature and then for 12 h at 105°C in a vacuum oven. Absolutely dried specimens were then set in a closed box, the air replaced with dried nitrogen, and  $E'$  and  $\tan\delta$  of specimens were measured at 20°C. Next, the relative humidity in the box was increased by steps to 3%, 11%, 33%, 58%, 75%, 85%, 95%, 97%, and 100% using dried silica gel or salt solutions<sup>14</sup> and further measurements carried out after 2 weeks of conditioning at each humidity.

## RESULTS AND DISCUSSION

### Moisture dependence of $E'$ and $\tan\delta$

*Table 1* lists  $\omega$ , angular frequency  $\omega = 2\pi f$ ,  $E'$ , and  $\tan\delta$  at various moisture contents (M).  $E'$  and  $\tan\delta$  are plotted against M in *Figure 2*.  $E'$  showed a peak at around 3%

\* To whom correspondence should be addressed

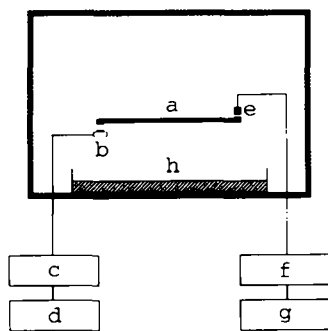


**Figure 1** Apparatus for the measurement of dynamic Young's modulus and loss tangent: (a) specimen, (b) vibrating magnet, (c) amplifier, (d) generator, (e) transducer, (f) band pass filter, (g) FT analyzer, (h) salt solution for humidity control

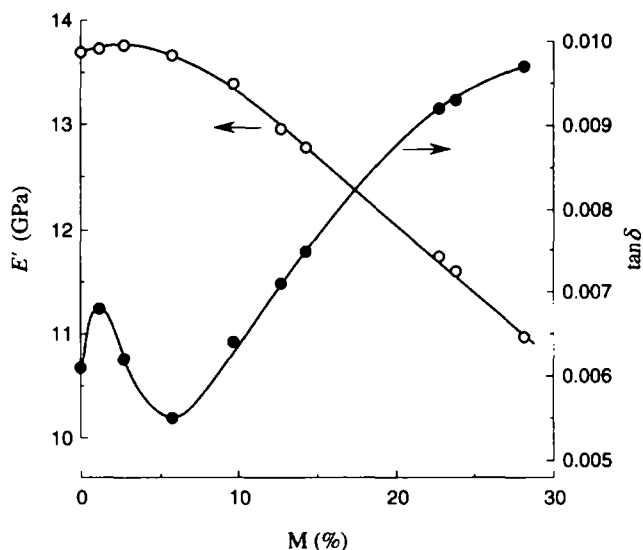


**Figure 2** The storage modulus ( $E'$ ) and the loss tangent ( $\tan\delta$ ) of spruce wood specimen in the longitudinal direction at 20°C plotted against moisture content (M)

**Table 1** Specific gravities ( $\gamma$ ), resonant angular frequencies ( $\omega$ ), storage modulus ( $E'$ ), loss tangent ( $\tan\delta$ ) of spruce wood at various moisture contents (M)

M(%)	$\gamma$	$\omega$	$E'$ (GPa)	$\tan\delta$
0.0	0.422	2749	13.69	0.0061
1.2	0.426	2753	13.72	0.0068
2.7	0.429	2758	13.76	0.0062
5.8	0.435	2752	13.66	0.0055
9.6	0.443	2730	13.39	0.0064
12.7	0.448	2691	12.95	0.0071
14.2	0.451	2675	12.78	0.0075
22.8	0.466	2581	11.73	0.0092
23.8	0.468	2567	11.59	0.0093
28.1	0.474	2508	10.97	0.0097

moisture content. Such a peak has been reported for wood and cotton<sup>15</sup>, but for a different value of M. It must be noted that the change of  $E'$  reflects the swelling contribution of matrix as well as its structural changes.

$\tan\delta$  had a relative maximum at about 1% moisture content. Such a peak was observed at 4% moisture content, -18°C and 2–3 kHz by James<sup>3</sup>, and at 3% moisture content, 25–30°C and 50 kHz by Suzuki<sup>4</sup>. Suzuki attributed this to the interaction between wood and adsorbed water. Figure 3 shows the temperature dependence of the storage modulus and the loss modulus ( $E''$ ) of spruce wood with various

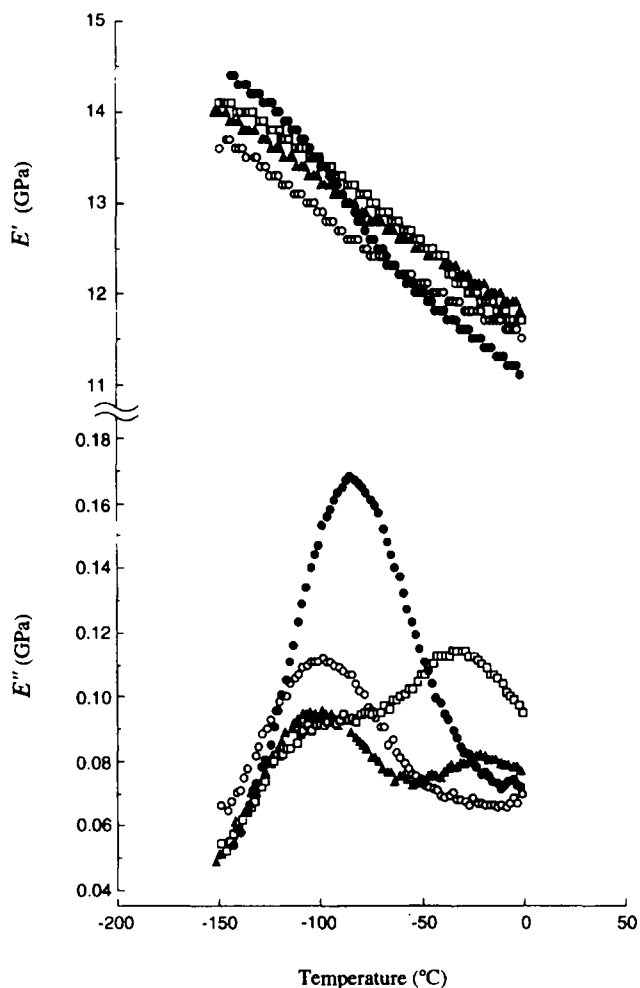


**Figure 3** The storage modulus ( $E'$ ) and the loss modulus ( $E''$ ) of spruce wood specimens in the longitudinal direction plotted against temperature<sup>16</sup>: (○) absolutely dry, (▲) 0.5% moisture content (M), (□) 0.7% M, (●) 3.2% M

moisture contents in the longitudinal direction<sup>16</sup>. A loss peak due to the motion of adsorbed water was observed at around -40°C and 33 Hz in the specimens containing a small amount of water. This peak shifted to a lower temperature with increasing M. From these results, the  $\tan\delta$  peak at around 1% moisture content was attributed to the motion of the adsorbed water. Similar results have reported in cellulose<sup>17</sup> and other polymers<sup>18–20</sup>. Above 6% moisture content,  $\tan\delta$  increased with increasing M.

*Uniaxial modelling of the cell wall*

We tried to estimate the intrinsic dynamic properties of matrix by using a mechanical model to eliminate the contribution of the swelling. Figure 4a shows a schematic structure of the wood cell wall. As the mechanical properties of the cell wall in the longitudinal (L) direction are mainly governed by those of the thickest  $S_2$  layer, we adopted the simple cell wall model shown in Figure 4b. As the first approximation, the Young's modulus of the model in the L direction can be expressed by

$$E_L = \left[ \frac{1}{E_1} \cos^4\theta + \left( \frac{1}{G} - \frac{2\mu_{12}}{E_1} \right) \sin^2\theta \cos^2\theta + \frac{1}{E_2} \sin^4\theta \right]^{-1} \quad (1)$$

where  $\theta$ (rad) is the mean fibril angle of the  $S_2$  layer,  $E_1$  and  $E_2$  are the Young's moduli in the 1 and 2 directions,  $G$  is the

shear modulus in the 1-2 plane, and  $\mu_{12}$  is the Poisson's ratio, respectively. As  $\mu_{12}$  is small enough to neglect  $2\mu_{12}/E_1$  compared to  $1/G'$ , and  $\theta$  is small enough to ensure  $\cos^4\theta \approx 1$ ,  $\sin^2\theta\cos^2\theta \approx \theta^2$  and  $\sin^4\theta \approx 0$ , equation (1) is approximately expressed by

$$E_L \approx \left( \frac{1}{E_1} + \frac{\theta^2}{G'} \right)^{-1} \quad (2)$$

In linear viscoelastic media, equation (1) or equation (2) remain valid when replacing static rigidities or compliance by their corresponding complex values, so that the complex Young's modulus in the L direction  $E_L^*(=E_L' + iE_L'')$  is related to the quantities  $E_1^*(=E_1' + iE_1'')$  and  $G^*(=G' + iG'')$  by

$$E_L^* \approx \left( \frac{1}{E_1^*} + \frac{\theta^2}{G^*} \right)^{-1} = \left( \frac{1}{E_1' + iE_1''} + \frac{\theta^2}{G' + iG''} \right)^{-1} \\ \approx \left[ \frac{1}{E_1'} + \frac{\theta^2}{G'} - i \left( \frac{E_1''}{E_1'^2} + \frac{\theta^2 G''}{G'^2} \right) \right]^{-1} \quad (3)$$

where it must be recalled that, in the time-temperature domain calculated here for wood, imaginary parts can always be considered as much smaller than the real parts. The real and imaginary parts of  $E_L^*$  are

$$E_L' \approx \left( \frac{1}{E_1'} + \frac{\theta^2}{G'} \right)^{-1}, \\ E_L'' \approx \left( \frac{E_1''}{E_1'^2} + \frac{\theta^2 G''}{G'^2} \right) \left( \frac{1}{E_1'} + \frac{\theta^2}{G'} \right)^{-2} \quad (4)$$

The storage modulus  $E'$  and the loss tangent  $\tan\delta$  of wood in the L direction are expressed by

$$E_L' \approx \frac{\gamma^v}{\gamma_w} E_L' \approx \frac{\gamma^v}{\gamma_w} \left( \frac{1}{E_1'} + \frac{\theta^2}{G'} \right)^{-1}, \quad (5)$$

$$\tan\delta \approx \left( \frac{E_1''}{E_1'^2} + \frac{\theta^2 G''}{G'^2} \right) \left( \frac{1}{E_1'} + \frac{\theta^2}{G'} \right)^{-1} \quad (6)$$

where  $\gamma$  is the specific gravity of specimen,  $v$  the volume fraction of the  $S_2$  layer in the cell wall, and  $\gamma_w$  the specific gravity of the cell wall.

Next we want to relate those equations to local quantities of the cell wall constituents. The  $S_2$  layer consists of two phases, elastic fibrils and viscoelastic matrix. They are almost in parallel along the axial direction of fibrils (the 1 direction), as shown in Figure 4b. The complex Young's modulus  $E_1^*$  is given by

$$E_1^* = \psi E_f + (1 - \psi)(E_m + iE_m'') \\ = |\psi E_f + (1 - \psi)E_m| + i(1 - \psi)E_m'' \\ = |\psi E_f + (1 - \psi)E_m| + i(1 - \psi)E_m \tan\delta_1.$$

Therefore, assuming  $E_m/E_f < 1$ ,

$$E_1' \approx \psi E_f$$

and

$$E_1'' \approx (1 - \psi)E_m \tan\delta_1 \quad (7)$$

where  $E_f$  is the Young's modulus of fibrils in the 1 direction,  $E_m^*(=E_m + iE_m'')$  is the complex Young's modulus of

matrix,  $\psi$  is the volume fraction of fibrils in the cell wall, and  $\tan\delta_1(=E_m''/E_m)$  is the loss tangent of matrix in the 1 direction. In the model shown in Figure 4c, fibrils with square cross-sections are embedded in matrix, so that fibrils and matrix are aligned partly in series and partly in parallel to the direction of shear force. According to the law of mixtures<sup>21</sup> and assuming  $G_m/G_f \ll 1$ , the complex shear modulus  $G^*$  is given by

$$G^* \approx G_m \left( 1 + \frac{\psi}{1 - \sqrt{\psi}} \right) (1 - A) \\ + iG_m \left( 1 + \frac{\psi}{1 - \sqrt{\psi}} \right) (1 - 2A) \tan\delta_6$$

where

$$A = \frac{\psi}{(1 - \sqrt{\psi})(1 - \sqrt{\psi} + \psi)} \frac{G_m}{G_f} \ll 1,$$

and therefore,

$$G' \approx G_m \left( 1 + \frac{\psi}{1 - \sqrt{\psi}} \right), \text{ and} \\ G'' \approx G_m \left( 1 + \frac{\psi}{1 - \sqrt{\psi}} \right) \tan\delta_6 \quad (8)$$

where  $G_f$  is the shear modulus of fibrils in the 1-2 plane,  $G_m^*(=G_m + iG_m'')$  is the complex shear modulus of matrix in the 1-2 plane, and  $\tan\delta_6(=G_m''/G_m)$  is the loss tangent of matrix in shear.  $E'$  and  $\tan\delta$  of the model are obtained by combining equations (5)-(8).

In the present range of frequency and temperature the matrix can be assumed to be in a glassy state, and the coefficient of viscosity is given by the following expression,

$$\eta_m \approx \frac{E_m}{\omega \tan\delta_m} \quad (9)$$

where  $\omega$  is the angular frequency, and  $\tan\delta_m$  is the loss tangent of the matrix.

An experimental value of 0.84 was adopted for equation (7). A value of 0.087 rad ( $5^\circ$ ) for  $\theta$  was estimated from the experimental relationship between  $E'/\gamma$  and  $\theta$ <sup>22</sup>. The values of  $\gamma_w$  and  $\psi$  were calculated from M in the following way. The volume fractions of cellulose, hemicellulose and lignin of absolutely dry wood were derived from weight fractions and specific gravities<sup>23</sup> (0.45 and 1.55 for cellulose, 0.30 and 1.47 for hemicellulose, 0.25 and 1.34 for lignin, respectively).  $\psi = 0.576$  was estimated by assuming that half of all hemicellulose is in the fibrils. The adsorption of water in the cell wall induces the swelling of the matrix.  $\gamma_w$  and  $\psi$  at different M were calculated by considering that the specific gravity of adsorbed water is 1 and the volume of cell lumen remains unchanged<sup>24</sup>.

Many theoretical values of Young's modulus for cellulose microfibrils or crystal have been reported<sup>25-28</sup>. However, these values were substantially different with one another, depending on the adopted models and assumptions. Therefore, an experimental value of 134 GPa for  $E_f$  was adopted, the value of which was determined from the X-ray measurement of cellulose crystalline lattice extension at various stress levels by Sakurada *et al.*<sup>29</sup>.

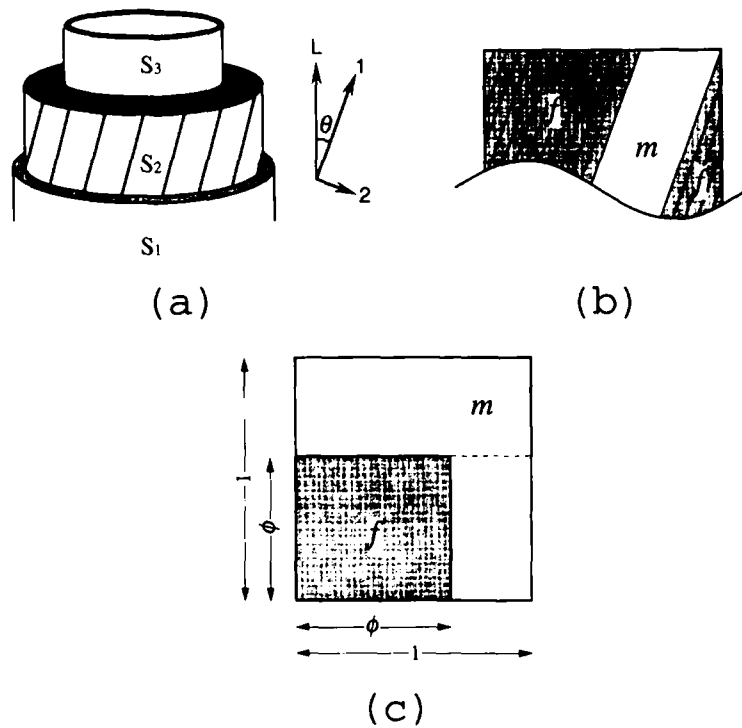


**Figure 4** Schematic model for analogies: (a) cell wall structure, (b) side view of  $S_2$  layer, (c) cross-section of  $S_2$  layer:  $L$  = longitudinal direction of wood,  $1$  = direction of fibril axis in  $S_2$  layer,  $2$  = direction perpendicular to  $1$  direction,  $\theta$  = fibril angle to  $L$  direction,  $f$  = cellulosic fibrils,  $m$  = amorphous matrix substance,  $\phi$  = side length of fibrils

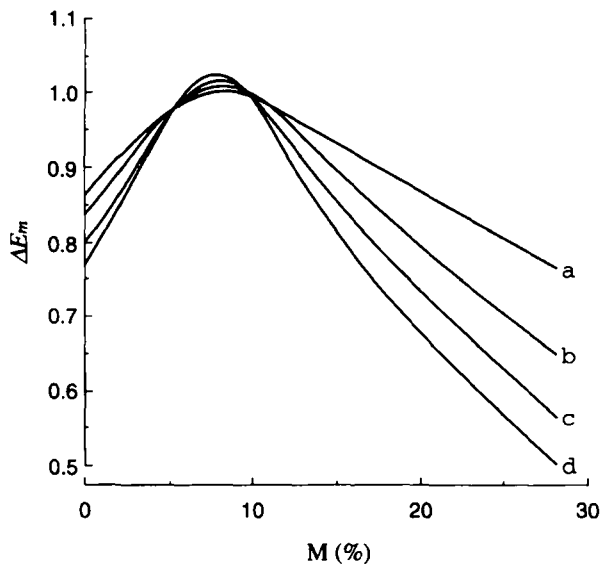


**Figure 5** The relationship between the normalized Young's modulus of matrix substance ( $\Delta E_m$ ) and moisture content ( $M$ ) for various values of  $p$  and  $q$ : (a) ( $p, q$ ) = (0.5, 2.0), (b) (1.0, 1.0), (c) (1.5, 0.7), (d) (2.0, 0.5)

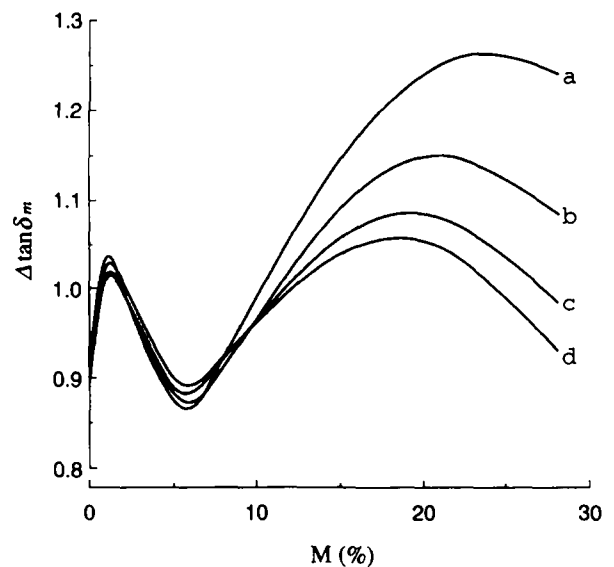


**Figure 6** The relationship between the normalized loss tangent of matrix substance ( $\Delta \tan \delta_m$ ) and moisture content ( $M$ ) for various values of  $p$  and  $q$ . Legend shown in Figure 5

Srinivasan<sup>30</sup> obtained a value of 2 GPa for the Young's modulus of isolated lignin. Cousins<sup>31</sup> measured the Young's modulus and shear modulus of isolated lignins which were 2.7~4.0 GPa and 1.2~1.5 GPa at 60% relative humidity, respectively. This result suggests that lignin is isotropic. Mark regarded the Young's modulus of isolated lignin as the best available approximation to that for matrix and adopted a value of 2 GPa for  $E_m$  and a value of 0.77 GPa for  $G_m$  by assuming the isotropy of matrix substance. In this paper, Mark's estimates for  $E_m$  and  $G_m$  adopted by many authors were used.

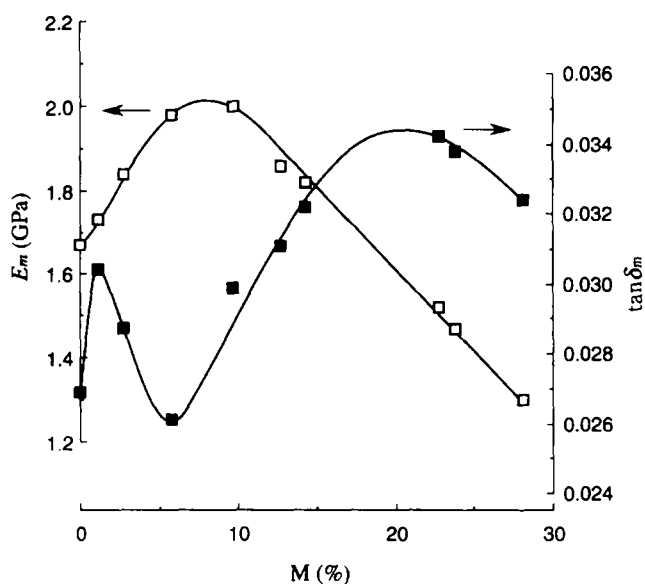
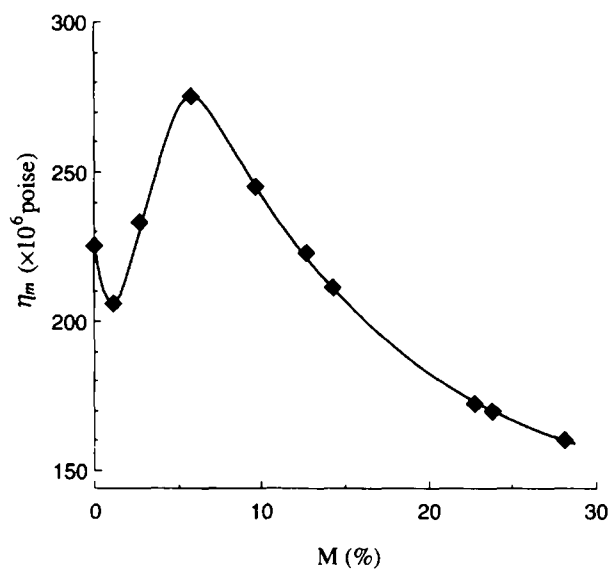
There is no experimental value for the loss tangent of

matrix ( $\tan \delta_m$ ). Our previous paper<sup>32</sup> showed an excellent negative correlation, depending on the mean microfibril angle, between  $\log E'/\gamma$  and  $\log \tan \delta$  for wood at 60% relative humidity. From this regression line, the value of  $\tan \delta$  for the model was estimated, and then a value of 0.0299 was calculated from equations (6)–(8) by assuming isotropic matrix and  $\tan \delta_m = \tan \delta_1 = \tan \delta_6$ . However, there is a possibility that the matrix substance is anisotropic to some extent<sup>33</sup>, so that the influence of the anisotropy of matrix on the relationship between  $E_m$  or  $G_m$  and  $M$  was examined.

By using constants described above, the  $G'$  value of the

**Table 2** The calculated values of volume fraction of fibrils ( $\psi$ ), specific gravities of cell wall ( $\gamma_w$ ), Young's modulus ( $E_m$ ), shear modulus ( $G_m$ ), loss tangent ( $\tan\delta_m$ ), and coefficient of viscosity ( $\eta_m$ ) of matrix at respective moisture contents (M)

M(%)	$\psi$	$\gamma_w$	$E_m$ (GPa)	$G_m$ (GPa)	$\tan\delta_m$	$\eta_m$ ( $10^6$ poise)
0.0	0.576	1.47	1.67	0.642	0.0269	225
1.2	0.566	1.46	1.73	0.665	0.0304	206
2.7	0.554	1.45	1.84	0.710	0.0287	233
5.8	0.531	1.43	1.98	0.763	0.0261	276
9.6	0.505	1.41	2.00	0.770	0.0299	245
12.7	0.486	1.39	1.86	0.718	0.0311	223
14.2	0.477	1.39	1.82	0.701	0.0322	212
22.8	0.432	1.35	1.52	0.585	0.0342	172
23.8	0.427	1.35	1.47	0.567	0.0338	170
28.1	0.408	1.33	1.30	0.501	0.0324	160


**Figure 7** The Young's modulus ( $E_m$ ) and the loss tangent ( $\tan\delta_m$ ) of matrix substance plotted against moisture content (M)

**Figure 8** The coefficient of viscosity of matrix substance ( $\eta_m$ ) plotted against moisture content (M)

$S_2$  layer at 60% relative humidity predicted from the model was 2.1 GPa, which was comparable with the average experimental value of 1.9 GPa for the wood cell wall<sup>34,35</sup>. Further, the values of  $E'$  and  $\tan\delta$  derived from the model were 14.35 GPa and 0.0062, respectively, which were close to the experimental values of 13.39 GPa and 0.0064.

$E_m$ ,  $G_m$  and  $\tan\delta_m$  at various moisture contents were estimated by assuming that  $E_m$  varies in proportion to  $G_m$ , and the calculated values of  $E'$  and  $\tan\delta$  change with moisture content in proportion to the experimental values. The values of  $\gamma_w$ ,  $\psi$ ,  $E_m$ ,  $G_m$ ,  $\tan\delta_m$  and  $\eta_m$  at various moisture contents led from  $\gamma$ ,  $E'$ , and  $\tan\delta$ , are listed in Table 2.

### Discussion

The aim of this study is to clarify the moisture dependence of  $E_m$  and  $\tan\delta_m$  in relation to structural changes in the matrix. Before considering a result, the influence of the anisotropy of matrix on the moisture dependence of  $E_m$  and  $\tan\delta_m$  was examined. The anisotropy of matrix was expressed by the following equations.

$$G_m = p \frac{1}{2(1+\mu)} E_m \approx \frac{p}{3} E_m, \quad \tan\delta_6 = q \tan\delta_1 \quad (10)$$

where  $\mu$  is the Poisson's ratio. Figures 5 and 6 show the moisture dependence of the normalized  $E_m$  and  $\tan\delta_m$ . The peak locations of  $E_m$  and  $\tan\delta_m$  remained unchanged regardless of values of  $p$  and  $q$ ; thus, it is possible to

discuss the peak location by assuming that the matrix is isotropic.

$E_m$  and  $\tan\delta_m$  at  $p = q = 1$  (isotropic) are plotted against M in Figure 7.  $E_m$  reached a maximum value at around 8% moisture content. The  $E'$  peak in Figure 2 was shifted to a higher moisture content by eliminating the swelling contribution of matrix. We next considered the effects of adsorbed water on the viscoelastic properties of matrix. It is speculated that in absolutely dry wood, intermolecular hydrogen bonds form in the distorted state and some adsorption sites remain 'open'. When a small amount of water is adsorbed, the molecular chains are then rearranged with the scission of hydrogen bonds formed in the distorted state. This explanation may account for the  $E_m$  peak. In our previous study<sup>36</sup>, the water sorption isotherms of spruce wood were analysed by the Hailwood-Horrobin adsorption equation<sup>37</sup>, and the adsorbed water was separated into hydrated and dissolved water. The results showed that the sorption sites were occupied mostly by the hydrated water below 8% moisture content and the dissolved water increased rapidly above 8% moisture content. The dissolved water was considered to decrease  $E_m$  by plasticizing matrix molecules.

$\tan\delta_m$  had two peaks at around 1% and 20% moisture content. The peak at 1% was due to the relaxation related to the motion of adsorbed water. Although Suzuki<sup>4</sup> suggested that  $\tan\delta$  peak was related to  $E'$  peak, the peak positions of  $E_m$  and  $\tan\delta_m$  were apparently different when the swelling

contribution was eliminated. This result suggested that  $E_m$  and  $\tan\delta_m$  peaks should be considered separately. The peak of  $\tan\delta_m$  at around 20% moisture content resembles the loss peaks detected using the torsion method<sup>5,6</sup>. Recently, Furuta *et al.*<sup>38</sup> found a relaxation process at 0.5 Hz and  $-40^\circ\text{C}$  for wood with 25% moisture content. They attributed it to the micro-Brownian motion of amorphous substances, especially hemicellulose. The observed peak at around 20% moisture content and room temperature may be related to that detected by Furuta *et al.*

$\eta_m$  is plotted against M in Figure 8. The initial decrease in  $\eta_m$  from 0 to 1% moisture content is considered to be due to the motion of adsorbed water itself. On the other hand, the peak of  $\eta_m$  at about 6% moisture content can be attributed to the rearrangement of matrix molecules as stated previously.

#### APPENDIX A:

Equation (8) is derived by using the mixture law as follows. In the  $S_2$  layer, fibrils and matrix are partly in series and partly in parallel to the shear force in the 1-2 plane as shown in Figure 4c. The reciprocal of the complex shear modulus of matrix is

$$\frac{1}{G_m^*} = \frac{1}{G_m + iG_m''} \approx \frac{1}{G_m} = i \frac{G_m''}{G_m^2}$$

The complex shear modulus for the series part ( $\bar{G}^*$ ), is

$$\bar{G}^* = \frac{1}{B - iC} \approx \frac{1}{B} + i \frac{C}{B^2}$$

where

$$B = \frac{\phi}{G_f} + \frac{1 - \phi}{G_m}$$

and

$$C = (1 - \phi) \frac{G_m''}{G_m^2}$$

$G_f$  and  $G_m$  at  $20^\circ\text{C}$  and 60% relative humidity are 4.4 GPa and 0.77 GPa, respectively<sup>7</sup>. Now with some approximation,

$$\frac{1}{B} = \frac{G_m}{1 - \phi} \frac{1}{1 + \frac{\phi}{1 - \phi} \frac{G_m}{G_f}} \approx \frac{G_m}{1 - \phi} \left( 1 - \frac{\phi}{1 - \phi} \frac{G_m}{G_f} \right),$$

and

$$\begin{aligned} \frac{1}{B^2} &= \frac{G_m^2}{(1 - \phi)^2} \frac{1}{\left( 1 + \frac{\phi}{1 - \phi} \frac{G_m}{G_f} \right)^2} \\ &\approx \frac{G_m^2}{(1 - \phi)^2} \left( 1 - \frac{2\phi}{1 - \phi} \frac{G_m}{G_f} \right). \end{aligned}$$

$G^*$  can be expressed by

$$\begin{aligned} G^* &= \phi \bar{G}^* + (1 - \phi)(G_m + iG_m'') \\ &\approx \frac{G_m}{1 - \phi} \left[ \phi \left( 1 - \frac{\phi}{1 - \phi} \frac{G_m}{G_f} \right) + (1 - \phi)^2 \right] \\ &\quad + i \frac{G_m''}{1 - \phi} \left[ \phi \left( 1 - \frac{2\phi}{1 - \phi} \frac{G_m}{G_f} \right) + (1 - \phi)^2 \right], \end{aligned}$$

when  $\phi^2 = \psi$ ,

$$\begin{aligned} G^* &\approx G_m \left( 1 + \frac{\psi}{1 - \sqrt{\psi}} \right) \\ &\quad \times \left[ 1 - \frac{\psi}{(1 - \sqrt{\psi})(1 - \sqrt{\psi} + \psi)} \frac{G_m}{G_f} \right] \\ &\quad + iG_m'' \left( 1 + \frac{\psi}{1 - \sqrt{\psi}} \right) \\ &\quad \times \left[ 1 - \frac{2\psi}{(1 - \sqrt{\psi})(1 - \sqrt{\psi} + \psi)} \frac{G_m}{G_f} \right] \end{aligned}$$

#### REFERENCES

- Kollmann, F. and Krech, H., *Holz als Roh-und Werkst.*, 1960, **18**, 41.
- Kadita, S., Yamada, T. and Suzuki, M., *Mokuzai Gakkaishi*, 1961, **7**, 29.
- James, W. L., *For. Prod. J.*, 1961, **11**, 383.
- Suzuki, M., *Mokuzai Gakkaishi*, 1962, **8**, 13.
- Norimoto, M. and Yamada, T., *Wood Res. and Tech. Note*, 1966, **38**, 32.
- Becker, H., Noack, D. and Reinbek, H., *Wood Sci. Tech.*, 1968, **2**, 213.
- Mark, R. E., *Cell Wall Mechanics of Tracheids*. Yale University Press, New Haven, CT, 1967.
- Mark, R. E. and Gillis, P. P., *Wood Fiber*, 1970, **2**, 79.
- Schniewind, A. P., in *Theory and Design of Wood and Fiber Composite Materials*, ed. B. A. Jayne. University of Washington, Seattle, WA, 1970.
- Tang, R. C. and Hsu, N. N., *Wood Fiber*, 1973, **5**, 139.
- Cave, I. D., *Wood Sci. Tech.*, 1978, **12**, 75.
- Akitsu, H., Gril, J. and Norimoto, M., *Mokuzai Gakkaishi*, 1993, **39**, 258.
- Hearmon, R. F. S., *Brit. J. Appl. Phys.*, 1958, **9**, 381.
- Yano, Y., *Handbook for Material and Water*. Kobunshi Gakkai, Kyoritsu Shuppan, Tokyo, 1968, p. 246.
- Wakeham, H. and Honold, E., *J. Appl. Phys.*, 1946, **17**, 698.
- Obataya, E., Yokoyama, M. and Norimoto, M., *Mokuzai Gakkaishi*, 1996, **42**, 243.
- Stratton, R. A., *Polym. Chem. Edition*, 1973, **11**, 535.
- Illers, K. H., *Macromol. Chem.*, 1960, **38**, 168.
- Woodward, A. E., Crissman, J. M. and Sauer, J. A., *J. Polym. Sci.*, 1960, **44**, 23.
- Bernier, G. A. and Kline, D. E., *J. Appl. Polym. Sci.*, 1968, **12**, 593.
- Takayanagi, H., Harima, H. and Iwata, Y., *Rpt. Prog. Polym. Phys. Jpn.*, 1963, **6**, 113.
- Norimoto, M., Tanaka, F., Ohogama, T. and Ikimune, R., *Wood Res. and Tech. Notes*, 1986, **22**, 53.
- Norimoto, M., Hayashi, S. and Yamada, T., *Holzforschung*, 1978, **32**, 167.
- Stamm, A. J., *Ind. Eng. Chem.*, 1938, **30**, 1280.
- Lyons, W. J., *J. Appl. Phys.*, 1959, **30**, 796.
- Treloar, L. R. G., *Polymer*, 1960, **1**, 290.
- Gillis, P. P., *J. Polym. Sci.*, 1969, **A2(7)**, 783.
- Jaswon, M. A., Gillis, P. P. and Mark, R. E., *Proc. Roy. Soc.*, 1968, **A306**, 389.
- Sakurada, I., Nukushina, Y. and Ito, T., *J. Polym. Sci.*, 1962, **57**, 651.
- Srinivasan, P. S., *Quart. J. Indian Inst. Sci.*, 1941, **4**, 222.
- Cousins, W. J., *Wood Sci. Tech.*, 1976, **10**, 9.
- Ono, T. and Norimoto, M., *Jpn. J. Appl. Phys.*, 1985, **24**, 960.
- Atalla, R. H. and Agarwal, U. P., *Science*, 1985, **227**, 636.
- Japanese Forest Experiment Station, *Handbook of Wood Industry*. Maruzen, Tokyo, 1982, p. 130.
- Ono, T., *J. Acoust. Soc. Jpn. (E)*, 1996, **17**, 183.
- Obataya, E. and Norimoto, M., *Mokuzai Gakkaishi*, 1995, **41**, 1079.
- Hailwood, A. J. and Horrobin, S., *Trans. Farad. Soc.*, 1946, **42B**, 84.
- Furuta, Y., Aizawa, H., Yano, H., and Norimoto, M., *Mokuzai Gakkaishi*, in press.